Journal of Biomechanics 83 (2019) 280–290

Contents lists available at ScienceDirect

Journal of Biomechanics

journal homepage: www.elsevier.com/locate/jbiomech
www.JBiomech.com

Comparison of platelet activation through hinge vs bulk flow in bileaflet mechanical heart valves

Mohammadali Hedayat [a], Iman Borazjani [a,b,*]

[a] Department of Mechanical and Aerospace Engineering, State University of New York at Buffalo, Buffalo, USA
[b] J. Mike Walker '66 Department of Mechanical Engineering, Texas A&M University, College Station, USA

ARTICLE INFO

Article history:
Accepted 3 December 2018

Keywords:
Platelet activation
Mechanical heart valve
Hinge flow
Gap size
Overset grid
Eulerian framework

ABSTRACT

Bileaflet mechanical heart valves (BMHVs) are prone to thromboembolic complications which are believed to be initiated by platelet activation. Platelets are activated by non-physiologic shear stresses in the bulk flow or the leakage/hinge flow, whose contributions has yet to be quantified. Here, the contribution of bulk and hinge flows to the activation of platelets in BMHVs is quantified for the first time by performing simulations of the flow through a BMHV and resolving the hinge by overset grids (one grid for the bulk flow and two for the hinge regions coupled together using one-way and two-way interpolation). It was found that two-way coupling is essential to obtain correct hinge flow features. The platelet activation through the hinge for two gap sizes (250 and 150 μm) is compared to the activation in the bulk flow using two platelet activation models to ensure the consistency of the observed trends. The larger gap has a higher total activation, but a better washout ability due to higher velocities. The maximum shear stress observed in the bulk flow (~320 dyne/cm^2) is much smaller than the hinge (~1000 dyne/cm^2). However, the total activation by the bulk flow is found to be several folds higher than by the hinge/leakage flow. This is mainly due to the higher flow rate of the bulk flow which exposes much more platelets to shear stress than the leakage flow.

1. Introduction

It is estimated that about 2.5% of the U.S. population suffers from heart valve defects (Iung and Vahanian, 2011) which leads to approximately 67,500 valve replacement surgeries each year (Clark et al., 2012). Several designs for mechanical heart valves have been proposed. Among those bileaflet mechanical heart valves (BMHVs) are the most widely used which account for approximately 30% of surgical heart valve replacements (Suri and Schaff, 2013). However, these valves are prone to high level of platelet activation, hemolysis and thrombus formation (Tang et al., 2005; Dumont et al., 2007), and thus far from ideal. It is believed that the thrombus formation is initiated by platelet activation due to non-physiological flow field and consequently elevated shear stress generated in BMHVs. This non-physiological flow is either generated by the hinge/leakage flow or the disorganized bulk flow by the leaflets/housing of BMHVs. Nevertheless, the contribution of hinge/leakage and bulk flows to platelet activation has yet to be quantified.

The importance of hinge design in BMHVs was first noticed because of the high thrombus formation rate in the Medtronic Parallel BMHVs (Ellis et al., 1996). Since then several in vitro experiments have been conducted to characterize the flow and address the thromboembolic potentials in BMHVs (Ellis et al., 2000; Leo et al., 2002; Manning et al., 2003; Simon et al., 2004; Leo et al., 2006; Jun et al., 2014a,b; Klusak et al., 2015; Zhang et al., 2016). Travis et al. (2001) and Fallon et al. (2006) showed a considerable difference in change or markers of platelet damage for different gap sizes. Leo et al. (2002) reported the gap size has a significant effect on the Reynolds shear stress (RSS) and strength of the leakage jet. In addition, they found that the regular gap size is less prone to thrombus formation in comparison to smaller or larger ones. Jun et al. (2014a) showed that the gap size has a significant influence on shear stress and washout potential of BMHVs. However, due to the small temporal and spatial scales and complex nature of the flow in the hinge region, these experiments provided limited information on the flow field in this region.

To compensate the above shortcomings and obtain further understanding about the flow field and platelet activation in the hinge region, numerical simulations have been performed (Yun et al., 2014b,a; Hanafizadeh et al., 2016; Kuan et al., 2015). Simon et al. (2010a) investigated the importance of gap size on

* Corresponding author at: Texas A&M University, Mechanical Engineering Department, College Station, TX, USA.
E-mail address: iman@tamu.edu (I. Borazjani).

https://doi.org/10.1016/j.jbiomech.2018.12.003
0021-9290/

the flow field (washout ability and shear stress) in BMHVs. Later, Simon et al. (2010b) compared the thrombogenic performance (in terms of red blood cell damage) of three different hinge designs using one-way interpolation of velocities form a large scale simulation (Borazjani et al., 2008). Yun et al. (2012) extended the work by Simon et al. (2010b) to model the platelets more realistically using a particle-based method. Although these simulations provided a better understanding of thromboembolic potential in the hinge region, they were focused on the hinge flow and did not compare the activation with the one from the bulk flow.

Several studies addressed the importance of systole phase on blood damage and platelet activation (Bluestein et al., 2004; Alemu and Bluestein, 2007; Morbiducci et al., 2009; Alemu et al., 2010; Yun et al., 2014a). These papers showed that the wake and vortical structures generated near the BMHV leaflets and housing can expose blood elements to a dynamic and elevated shear stress. However, the activation in systole was not compared against a control case to show its significance. Hedayat et al. (2017) showed that the activation by the bulk flow in BMHVs during systole is significant (several folds higher) relative to a bio-prosthetic heart valve as the control, but it was not compared against the activation by the hinge/leakage flow during diastole. Lamson et al. (1993) compared red blood cell damage (hemolysis) in an MHV during different phases of a cardiac cycle by running forward flow through an open valve and backward flow through a closed valve. They found the contribution of backward flow to hemolysis to be comparable with that of the forward flow. However, hemolysis does not directly translate to platelet activation (Yin et al., 2004; Hosseinzadegan and Tafti, 2017). Dumont et al. (2007) and later Xenos et al. (2010) evaluated platelet activation through two different BMHVs using the linear activation model during the systole and regurgitation flow phase by releasing particles separately in systole and diastole. None of them explicitly compared the total amount of platelet activation in each phase, but their results imply that the mean value of activation for platelets released during the forward phase is higher than the diastole. Nevertheless, the hinge area was not resolved in these simulations and the gap region was simulated by scaling down the valve geometry (Dumont et al., 2007; Xenos et al., 2010).

In this study, we address the open question of whether the bulk or the hinge flow plays a more important role in the poor thrombogenic performance of BMHVs in terms of shear-induced platelet activation using a well-validated numerical framework (Section 2). Shear-induced platelet activation is quantified using two well established activation models, i.e., the linear level of activation (Bluestein et al., 1997) and Soares (Soares et al., 2013) models, to show the consistency of the results to different activation models (Section 2). In order to address this multi-scale (aortic diameter ≈ 25.4 mm vs. the hinge gap ≈ 150 μm) problem, an overset grid (one grid for the bulk flow and two grids for the hinge regions) method is used. The significance of using two-way over one-way (which was the main strategy in previous works) coupling interpolation for the boundary condition for the hinge domain in the overset method is investigated (Section 3.1). In addition, the effect of hinge gap width on the hemodynamic performance of hinge geometry and the platelet activation in MHVs is tested for two different gap sizes (250 and 150 μm) (Section 3.2). Finally, the platelet activation in the bulk flow domain and the hinge region is quantified and compared in Section 3.3. In the end, the conclusion and limitations are stated.

2. Methods and materials

The numerical method has been extensively validated and thoroughly described in previous publications (Gilmanov and Sotiropoulos, 2005; Ge and Sotiropoulos, 2007; Borazjani et al., 2008; Borazjani, 2013; Asgharzadeh and Borazjani, 2017), which is briefly described below. The moving boundaries of the valve are handled using a sharp-interface immersed boundary method (Gilmanov and Sotiropoulos, 2005; Ge and Sotiropoulos, 2007) with an efficient ray-tracing algorithm and strongly-coupled fluid-structure interaction for the motion of the valves (Borazjani et al., 2008). In addition, an overset method (Borazjani et al., 2013) is used to provide a high spatial resolution (with the grid size of 15 μm in the hinge recess) near the hinge regions (Fig. 1). The boundary conditions on overset grid boundaries are obtained using both two-way and one-way coupling interpolation. In one-way interpolation, the boundary conditions of the hinge domains are interpolated from the velocities in the large-scale simulation (Borazjani et al., 2008) but the flow in the hinge domain does not affect the flow in the large-scale domain. In two-way interpolation, the boundary conditions in the hinge domains are interpolated from the large-scale domain while the region close to the hinge and leaflet gaps is blanked in the large-scale domain (Fig. 1) (this region is not solved in the large-scale domain but is solved in the hinge domain). The velocities for this blank region are interpolated from the hinge domains and given to the large-scale domain as boundary conditions.

The valves are placed as an immersed boundary in an idealized axisymmetric aorta geometry under a physiological flow condition (Borazjani et al., 2008; Dasi et al., 2007; Jun et al., 2014a). The hinge geometry is modeled approximately based on a 23 mm St. Jude Medical BMHV. The model has two semicircular leaflet ears which pivot in butterfly-shaped hinge recesses (Fig. 1). Two gap sizes of 250 μm (large gap) and 150 μm (regular gap) are used in this study for the hinge region while the b-datum gap is kept constant (200 μm) in all simulations. In addition, the gap between valve leaflets and housing is neglected in this study. The placement and the angle of leaflets and housing are exactly the same as previous bulk-flow simulations (Borazjani et al., 2008) and experiments (Dasi et al., 2007; Jun et al., 2014a). The simulations are carried out for one cycle and further validated against previous experiments as reported in the supplementary materials.

2.1. Platelet activation

Because each model of platelet activation is tuned for a specific experiment, as explained by Grigioni et al. (2004) and Sheriff et al. (2013), the model coefficients are not universal and change from experiment to experiment. To make sure that the conclusions are independent of the model, two activation models (the linear activation (Bluestein et al., 1997) and Soares model (Soares et al., 2013)) are used in this work. Linear activation model is simple and widely used, but does not consider dynamic shear. Soares model (Soares et al., 2013), which is based on the Platelet Activation State (PAS) (Jesty and Bluestein, 1999) for dynamic shear stress (Nobili et al., 2008; Sheriff et al., 2013; Soares et al., 2013), accounts for the transient nature of flow as well as loading rate and sensitization on platelet activation.

To incorporate the activation models in numerical simulations both Eulerian and Lagrangian (two-phase or infinitesimal particle approach) approaches can be used. Considering the normal range of platelets in artery vessels, which is 150,000–400,000 per cubic millimeter (Ross et al., 1988), billions of particles need to be calculated each second which is not computationally feasible. In this work, therefore, an Eulerian framework (Hedayat et al., 2017) is utilized which considers activation as a continuum quantity. Since the Soares model requires a non-zero initial activation level, a background level of 1% is used for this model. The details of the platelet activation models, their validation, and the sensitivity of

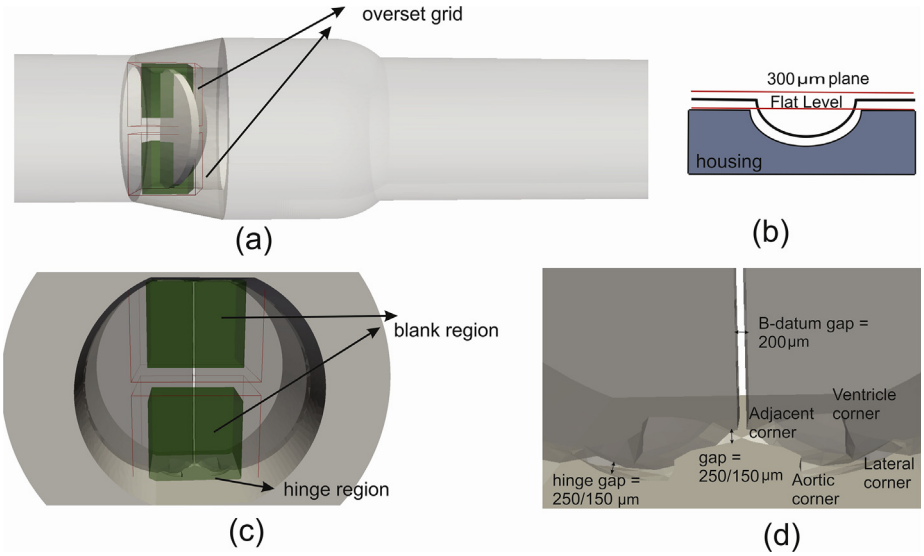

Fig. 1. (a) Large-scale domain for overset numerical simulation (b) flat level is chosen as the plane of reference (c) position of hinge domains and blank regions relative to hinge recess (d) hinge model with butterfly hinge recess.

the results to the initial activation in the Soares model is reported in the supplementary materials.

3. Results and discussion

In Section 3.1, the influence of interpolation method (one-way and two-way coupling) is investigated on the numerical results compared to the experimental ones. In Section 3.2, the effect of hinge gap size is investigated on the flow characteristics and platelet activation in the hinge region. Finally, the platelet activation in the bulk flow is compared to the activation in the smaller hinge gap size (150 μm) using Soares and linear level of activation models (Section 3.3). The flat level (the plane where the semicircular hinge recess reaches the flat surface of housing) as well as the plane 300 μm above it for the hinge domain (Fig. 1), and mid-plane normal to $x-axis$ for the bulk flow are selected to visualize the results similar to previous experiments (Simon et al., 2004; Jun et al., 2014a). Since both activation models show the same trend, only the results of Soares model are shown here. The results for linear activation can be found in Section 3 of supplementary materials.

3.1. The interpolation method and comparison with experiments

Considering the small gap size of the hinge region and due to limitations in currently available computational resources, using

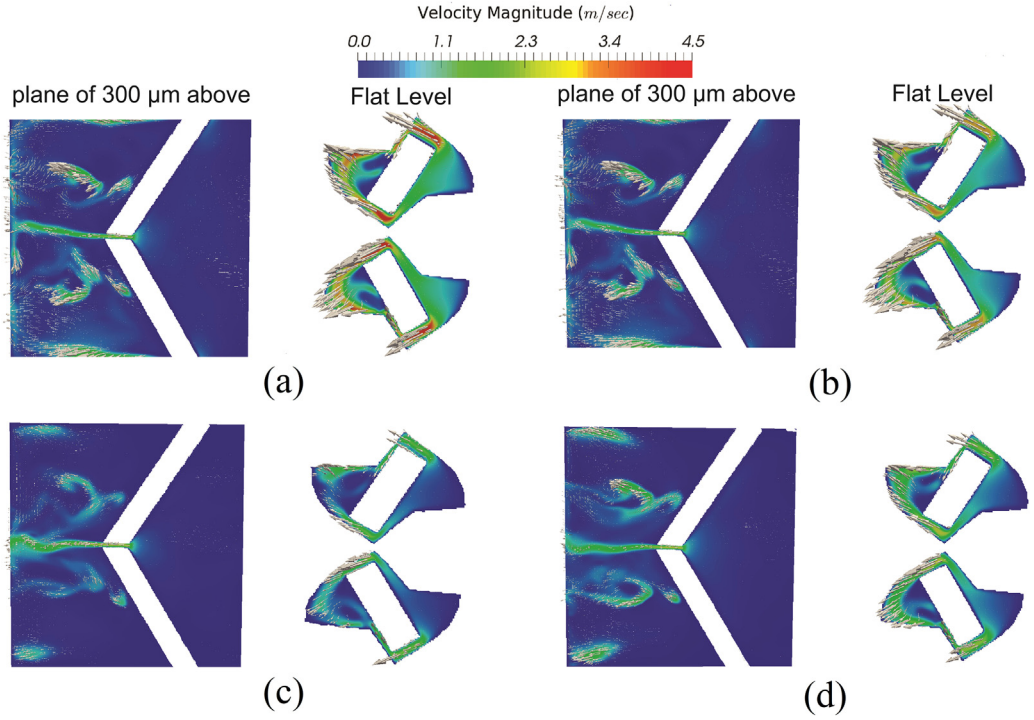

Fig. 2. Velocity contour and vectors for hinge domain at mid-diastole for different plane of view (a) one-way interpolation gap size of 150 μm (b) one-way interpolation gap size of 250 μm (c) two-way interpolation gap size of 150 μm (d) two-way interpolation gap size of 250 μm.

an overset grid (larger grid size for bulk flow and smaller mesh size for near the hinge region) seems inevitable (to keep good spatial and temporal resolutions) to perform a simulation through BMHVs in order to simultaneously capture the large and small-scale flow features. In previous works (Yun et al., 2012; Simon et al., 2010b, a), some simplifications were assumed for obtaining the boundary conditions of the domains near the hinge region. They extracted the velocity boundary conditions of small domains using one-way coupling interpolation from a large scale simulation (Borazjani et al., 2008) during the systole phase; while, for the diastole phase, they used a plug flow in a way to assure the pressure gradient of 80 mmHg across the valves at mid-diastole. As it will be shown later, the one-way coupling interpolation for velocities can lead to acceptable results during the systole phase. However, due to the disorganized nature of the flow during diastole phase assuming a plug backflow for the hinge domain is not that realistic.

Our results show that during the systole phase the scalar shear profile (Figs. 3 and 4) and the maximum magnitude of velocities on the flat plane (Fig. S7 of supplementary materials) are almost the same for both interpolations. However, the difference in velocity magnitude (through the hinge) due to interpolation is clearly visible during the diastole phase (Fig. 2a and c). Using one-way interpolation, at mid-diastole, the maximum velocity reaches 4.8 m/s and 3.6 m/s on the flat and 300 μm planes, respectively, in 150 μm hinge gap size. While using two-way interpolation, the maximum velocities of 2.4 m/s and 2.8 m/s is observed on the flat and 300 μm planes, respectively. The shear stress also changes drastically with the choice of interpolation during diastole. Fig. 3a shows the maximum shear stress observed using one-way interpolation is approximately two times higher than two-way interpolation (Fig.4a). Although the results of one-way interpolation (both maximum magnitude and glyph of velocity) are more close to the results of previous numerical simulations by Simon et al. (2010a), the maximum velocity (4.8 m/s) is very different from the maximum velocity observed in experiments by Simon et al. (2004) and Jun et al. (2014a) which is from 1.67 m/s to 3.1 m/s for different gap sizes. However, using two-way interpolation the maximum (2.8 m/s) and the velocity vectors are more close to the results of above experiments (see Fig. 8 of Jun et al. (2014a) and also Table 1).

Similarly, one-way interpolation overestimates the maximum shear stress (Table 1) and obviously the flux through the hinge region which can drastically affect the prediction of platelet activation in BMHVs. Fig. 5 compares the total activation, defined as the total amount of activation generated in the domain which is computed by the sum (integral) of platelet activation in the domain—see Eq. (12) in the supplementary materials, generated by the hinge region and b-datum gap during a cardiac cycle using Soares and linear models. The activation values in the figure are normalized by the total activation of the bulk flow at the end of the cardiac cycle in bulk flow. As it was mentioned during the systole

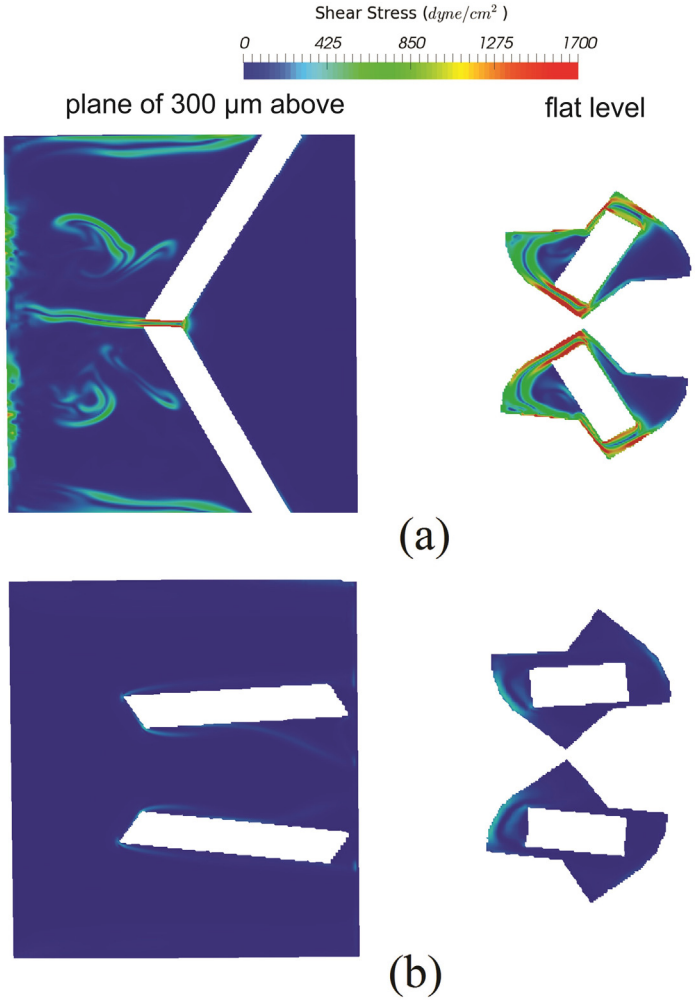

Fig. 3. Scalar shear stress for hinge domain using one-way interpolation for gap size of 150 μm for different plane of view (a) mid-diastole and (b) systole.

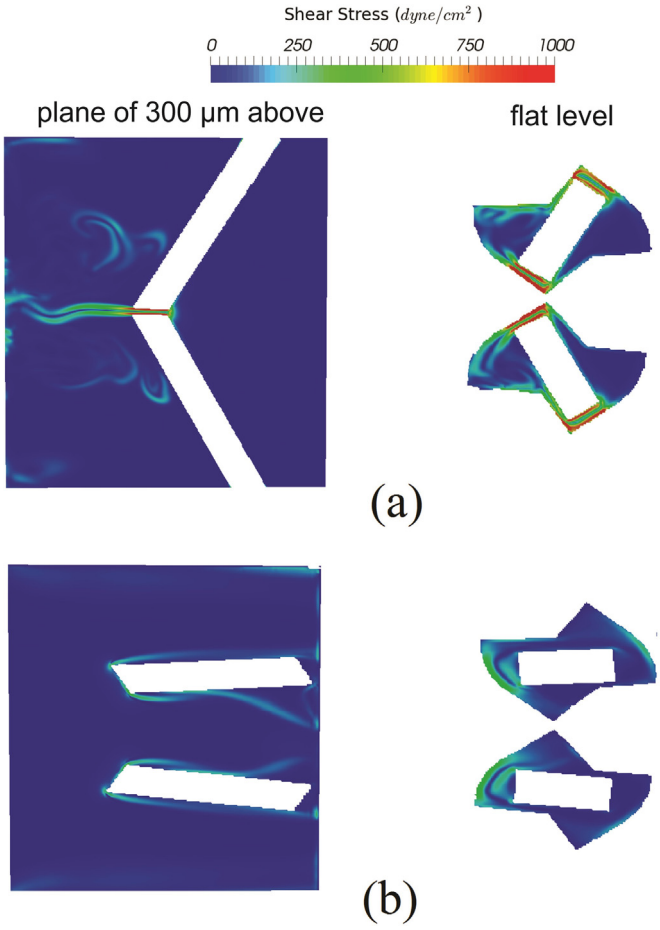

Fig. 4. Scalar shear stress for hinge domain using two-way interpolation for gap size of 150 μm for different plane of view (a) mid-diastole and (b) systole.

phase the one-way interpolation provides reasonable results in the hinge region. Thus, the total activation of one-way coupling is the same as the two-way one during systole in the hinge area. During diastole, however, the one-way interpolation generates much higher activation (more than two times) than the two-way interpolation for all gap sizes using both activation models. In addition, in one-way interpolation the total platelet activation of the smaller (150 μm) gap is higher than the larger one by approximately 50% and 35% (Fig. 5) using Soares and linear models, respectively, whereas two-way interpolation shows the opposite trend, i.e., the total activation the larger gap size is higher than the smaller one by 8% and 12% (Fig. 5) using Soares and linear activation models, respectively. The trend for the two-way interpolation is consistent with experimental results of Travis et al. (2001) and Leo et al. (2006) showing lower activation is associated with regular gap size (100 μm) compared to a larger one (200 μm). Because of the overestimation of velocities, shear stress, and the total activation of the one-way coupling relative to the experiments, one-way coupling is inadequate to obtain quantitative measures for activation in the hinge region. Therefore, we only discuss two-way coupling, whose results are close to previous experiments (Table 1 and 2 in supplementary materials), in the next sections.

3.2. Hinge flow and the gap size

The hinge gap width of BMHVs can vary due to manufacturing tolerance, or displacement of the leaflets, which can affect the flow in the hinge area. Our results show that the hinge gap size has a limited effect on the flow through the hinge during the systole phase, but it has a significant effect during the diastole in terms of velocity magnitudes which are directly related to washout ability in the hinge area (Fig. 2c, d). The maximum magnitude of the velocity on the flat level in the smaller gap is less (2.4 m/s) than the larger gap size (2.8 m/s). However, the magnitude of the b-datum jet does not change considerably for different gap sizes (~2.8 m/s). The change of hinge gap size mainly influences the flow in the ventricle corner. The maximum velocity in the ventricle corner reduces from 2.1 m/s in the larger gap size to 1.05 m/s in the smaller one. This smaller velocity suggests that the 150 μm gap size will have a weaker washout potential compared to the larger gap. The maximum shear stress observed in both gap sizes is in the same order of magnitude with a slightly higher shear stress in the larger gap size (1170 dyne/cm^2) in comparison to the smaller gap (1120 dyne/cm^2). The above trend for the shear stress and velocity magnitudes with the change in gap size is similar to the recent experiments of Jun et al. (2014a).

The results of platelet activation calculated using Soares model for larger and smaller gap sizes during the diastole phase are shown in Fig. 6. The maximum magnitude of platelet activation in both gaps is observed in ventricle corners. Furthermore, the activation contours show lower levels for the smaller gap than the larger one (Fig. 6). However, the activation due to the b-datum jet for

Table 1
Comparison of velocity and viscous shear stress at mid-diastole using different interpolation methods for current study to the previous experiments for 23 mm St. Jude Medical mechanical heart valve.

Source	Interpolation method	Gap size (μm)	Plane of view (μm)	Max velocity (m/s)	Max viscous shear stress (dyne/cm^2)
Simon et al. (2004)		100	Flat	1.75	–
		100	390	2.27	–
Jun et al. (2014a)		100	Flat	2.57	> 300
		100	390	2.52	> 300
		200	Flat	2.26	> 300
		200	390	2.91	> 300
Jun et al. (2014b)		Clinical	Flat	2.62	≈ 600
		Clinical	390	3.24	≈ 600
Current study	Two-way	150	Flat	2.38	1120
		150	300	2.85	1260
		250	Flat	2.65	1170
		250	300	2.78	1230
	One-way	150	Flat	4.83	1840
		150	300	2.63	1120
		250	Flat	3.9	1560
		250	300	2.71	1130

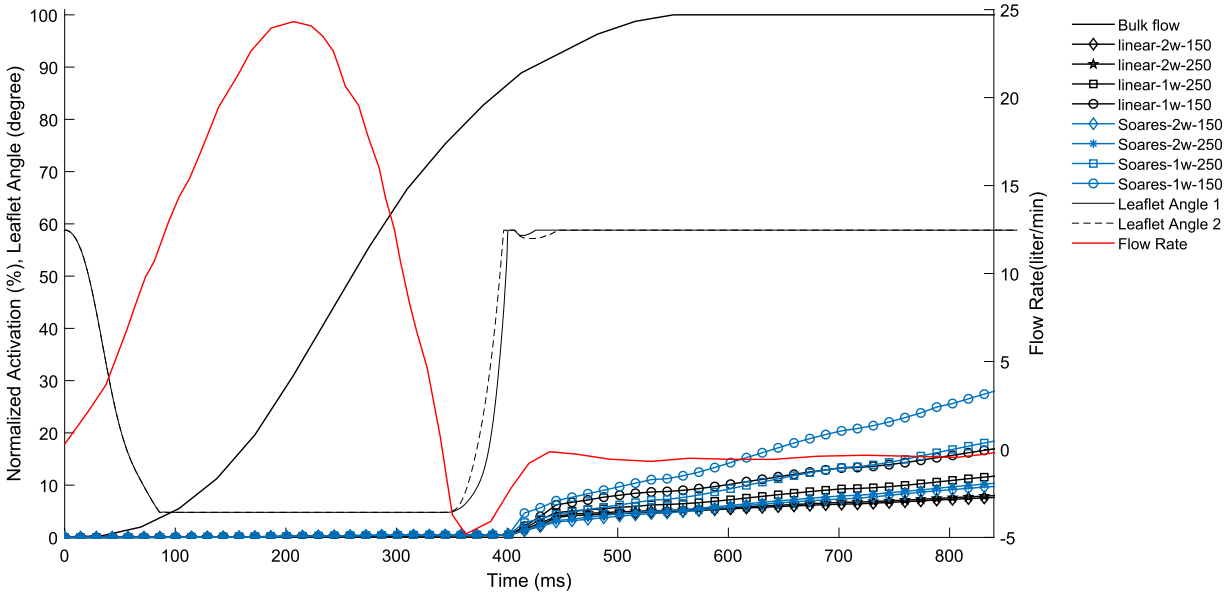

Fig. 5. Comparison of total platelet activation for the bulk and the hinge (for different gap sizes and interpolation models) flows using linear and Soares activation model within a cardiac cycle. The total activation is normalize by total activation of the bulk flow at the end of cycle for each model. The leaflet angles and the flow rates are also plotted. 1w and 2w denote one-way and two-way interpolation, respectively. 150 and 250 denote the gap size of the hinge region. Linear and Soares denote the platelet activation model.

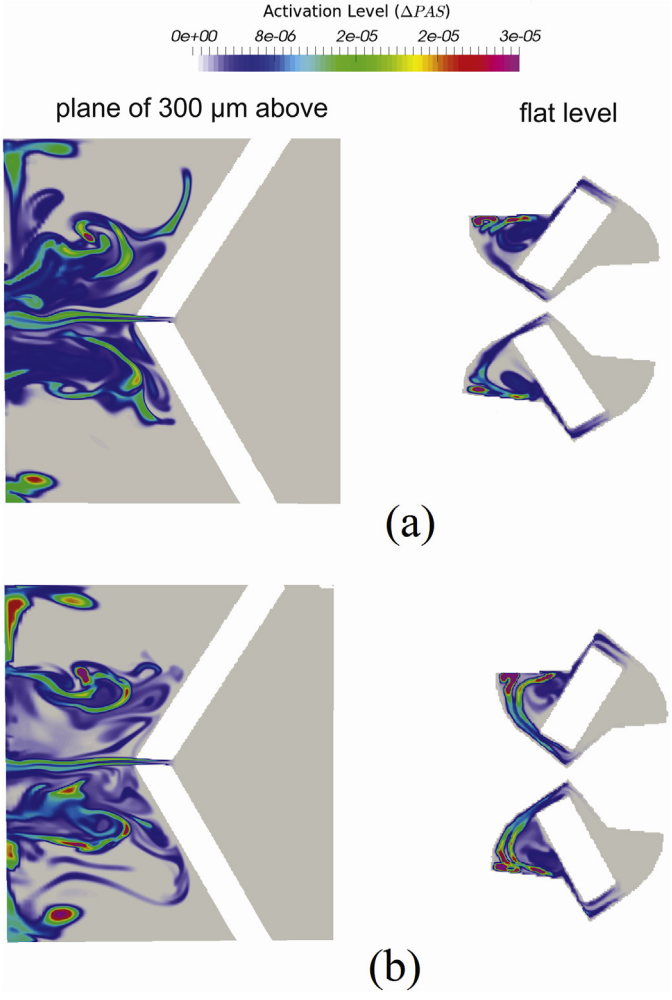

Fig. 6. Platelet activation of hinge domain using Soares model and two-way interpolation for both gap sizes At mid-diastole for different plane of view (a) gap size 150 μm and (b) gap size 250 μm.

different gap sizes shows no significant difference on the 300 μm plane. Comparing the total activation for different gap sizes by the two-way coupling in Fig. 5 shows that the total activation in the larger gap size is higher than the smaller one by 8% and 12% at the end of the cycle for linear and Soares models, respectively. This indicates that the larger gap size activates more platelets, which is consistent with the observation in the previous experiments (Travis et al., 2001).

3.3. Platelet activation in bulk versus hinge flow

To compare the impact of the bulk and hinge flow on the performance of BMHVs in terms of platelet activation, the total activation (Eq. (12) of supplementary materials) generated in each phase of the cardiac cycle is calculated. Fig. 5 compares the total platelet activation (activation production) caused by the hinge region and b-datum gap to the activation generated by the bulk flow during a cardiac cycle using Soares and linear activation models. As mentioned in the previous sections, the activation values in the figure are normalized by the total activation in the bulk flow at the end of the cycle (Eq. (13) of supplementary materials). Fig. 5 shows that the total activation at the end of the cycle generated by the bulk flow is several folds higher than the activation by the hinge region. In fact, the total activation of the hinge/leakage flow is only about 10% of the bulk flow for different gap sizes and the activation models. The reason for the higher total activation by the bulk flow will be closely examined below.

The trend of activation in Fig. 5 can be explained by the mechanics of activation. For the bulk flow, the total activation before mid-acceleration phase ($t = 100$ ms) is almost negligible because the vortical structures are well organized and symmetric (Fig. S2 of supplementary materials) which results in low shear stress (Fig. 7a) and platelet activation in the bulk flow (Fig. 8a). The rate of activation (slope of the line in Fig. 5) reaches its maximum at the peak systole ($t = 200$ ms) and this trend continues during the deceleration phase until the end of systole ($t = 360$ ms). The rate of total activation during the deceleration phase is higher (1.5 times) than the acceleration phase because

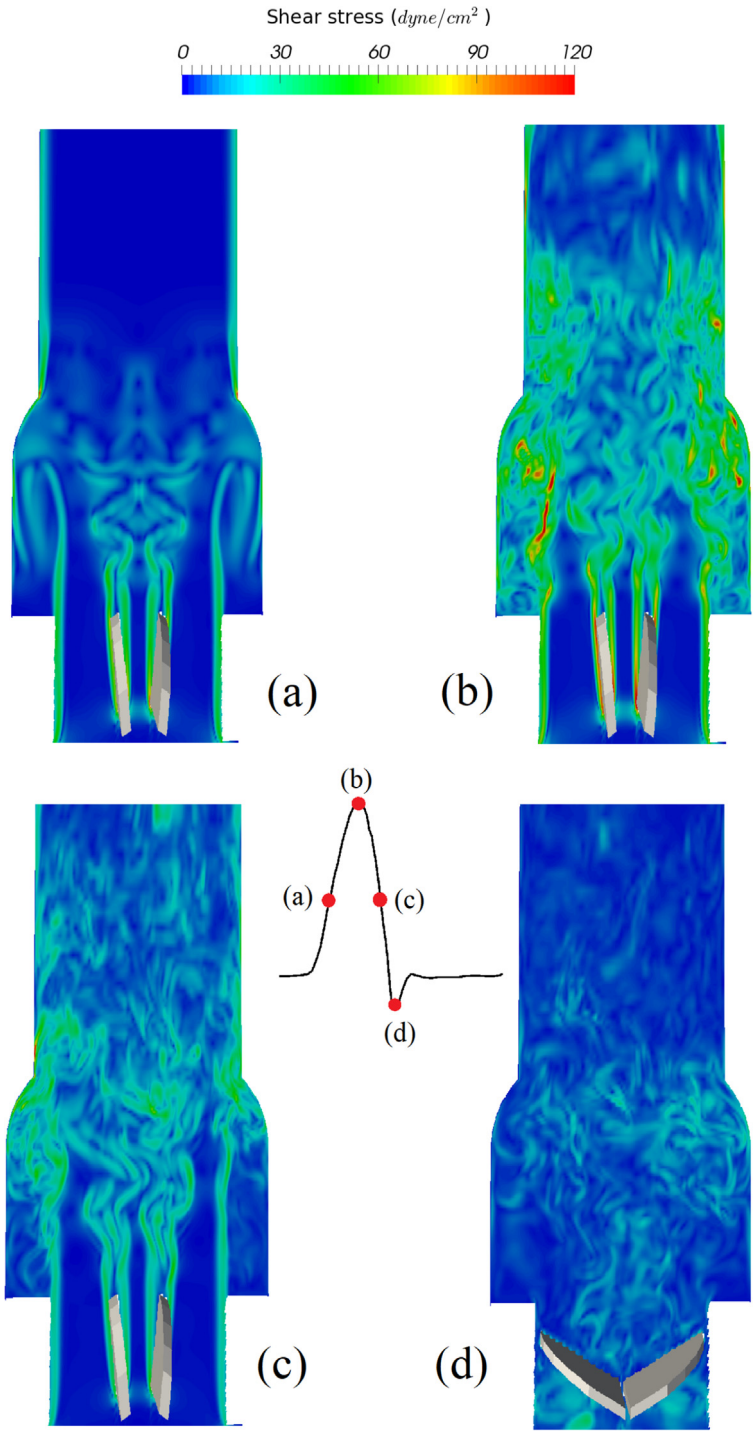

Fig. 7. Scalar shear stress for the MHV in the large-scale domain at time t = (a) 137, (b) 206, (c) 309, and (d) 412 ms within the cardiac cycle.

the vortical structures in the BMHV break down into small-scale disorganized vortices right before the peak systole (Fig. S2 of supplementary materials) similar to previous simulations and experiments (Dasi et al., 2007; Borazjani et al., 2008; Hedayat et al., 2017), which consequently generates regions of high shear stress (Fig. 7b–c) that activate platelets (Fig. 8b–c) during the deceleration phase. The activation in the bulk flow mainly happens during the systole phase, but platelet activation still occurs with a slower rate until $t = 550$ ms (Fig. 5) because of the small vortical structures remain in the flow (Figs. 7d, 8d) that slowly dissipate. Due to the dissipation of vortical structures in the bulk flow, after $t = 550$ ms the shear stress and consequently the activation production is negligible, i.e., total activation remains constant (Fig. 5).

For the hinge and b-datum gap at the beginning ($t < 80$ ms when the valves are opening) and the rest of systole the total activation is negligible (Fig. 5). This is interesting because the shear stress was not negligible during systole (Fig. 4) as discussed in the previous section. In fact, during the systole platelets may get activated due to the flow diving into the leaflet earrings and the hinge recess as shown by streamlines in Fig. 9b. The streamlines enter the hinge recess through the ventricular corner (from the gap between the

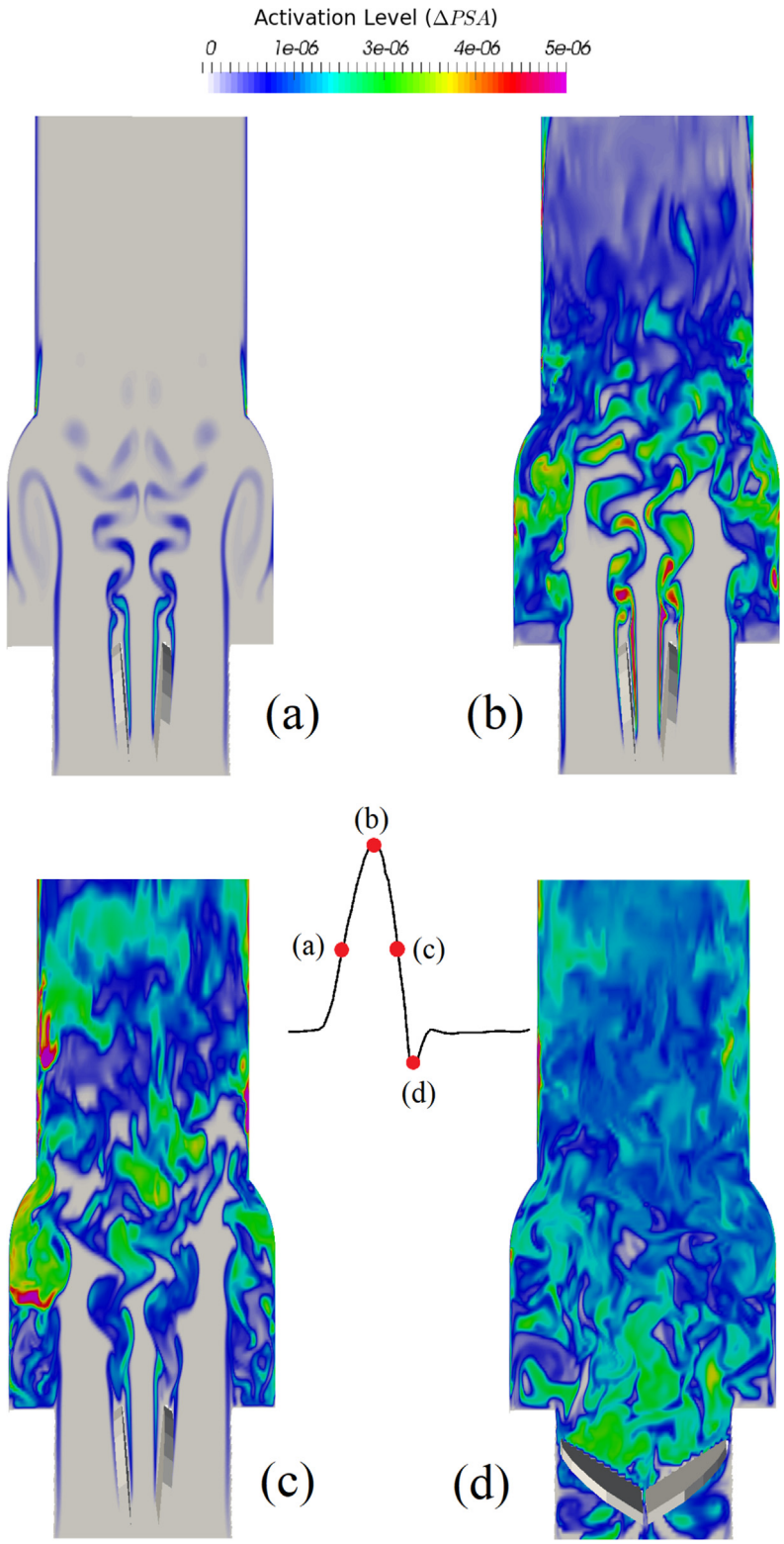

Fig. 8. Platelet activation for the MHV in the large-scale domain using the Soares activation model at time t = (a) 137, (b) 206, (c) 309, and (d) 412 ms within the cardiac cycle.

leaflet flat surface and housing) and exit through the adjacent and aortic corner. Two regions of high shear stress near the ventricle corner (between the flat level and leaflet surface) and near the adjacent corner can be observed in Fig. 4. However, the flow rate through this region during systole is small which can be seen by the magnitude of in-plane velocity (up to ≈0.5 m/s during the peak systole) on the flat level (Fig. 9c). Because of the small flow rate through the hinge recess, a lower number of platelets are exposed to high shear to get activated during systole, which renders the total activation of the hinge as negligible compared to the bulk flow.

The main activation in the hinge region and the b-datum gap happens during the diastole phase ($t = 400$ ms to $t = 860$ ms in

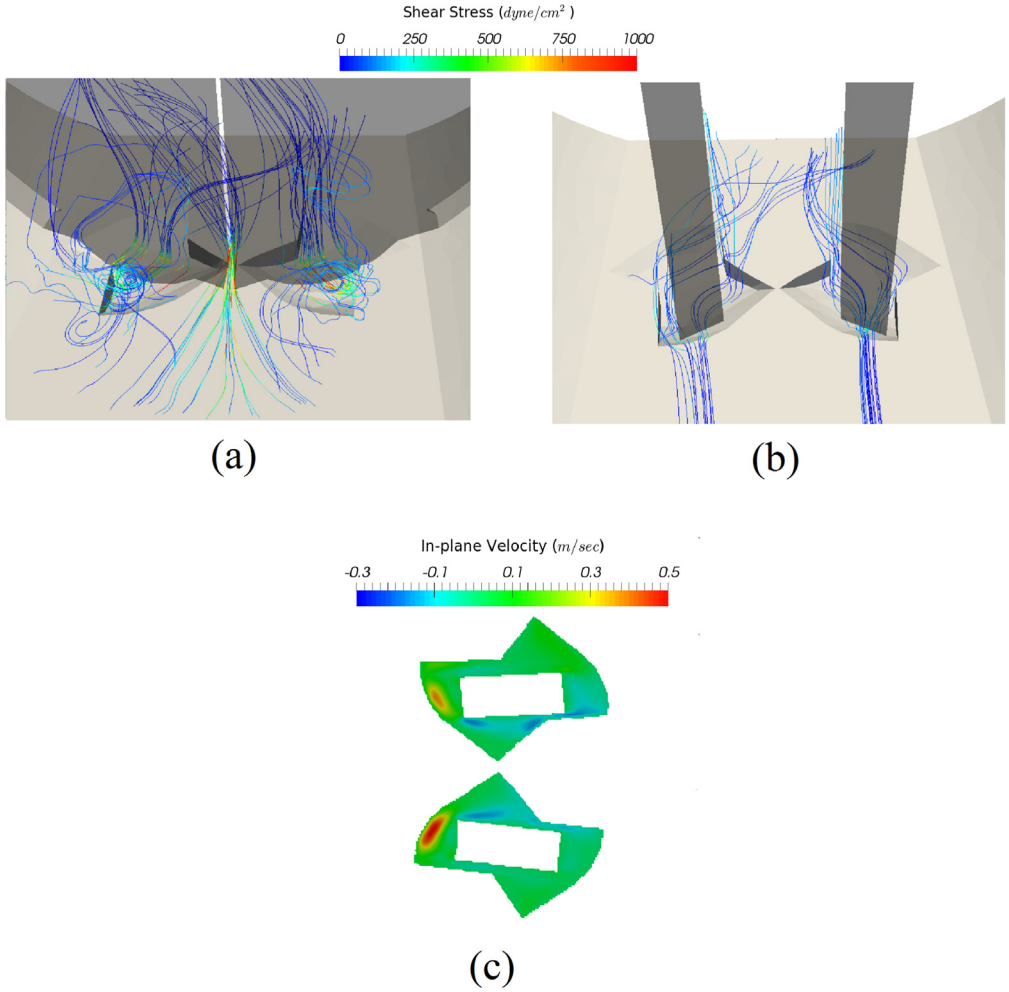

Fig. 9. Three-dimensional streamtraces at peak systole (a) and mid-diastole (b) for small-scale simulation near the hinge recess (c) In-plane velocity on the flat level at peak systole.

Fig. 5) because of the leakage flow through: (1) the gap between leaflet's earing and housing in the hinge recess; (2) the gap between the flat surface of leaflets and the housing; and (3) b-datum gap. These three gaps (Fig. 1 c) result in three leakage jets (Figs. 2c and 9a) which exit the hinge recess from lateral, adjacent and ventricle corners with the maximum velocity magnitude of 2.4 m/s (at the adjacent corner). The leakage jets create regions of high shear stress near these three corners with the maximum magnitude of 1120 dyne/cm^2 at the adjacent corner (Fig. 4a), which is much higher than the peak shear stress in the bulk flow ($\approx$ 200 dyne/cm^2). For the smaller gap size, the minimum of shear stress and velocity is observed in the ventricle corner. Fig. 6 shows the platelet activation at mid-diastole on the flat level using Soares activation model. A high magnitude of the activation is observed downstream of the valves near the ventricle corner. This can be explained by the streamtraces (Fig. 9a) in the hinge recess at mid-diastole (since the flow is almost steady in this phase the streamtracers and path-lines for platelets are almost the same). As it can be seen, due to the reverse flow, the streamlines dive into the hinge recess mostly from the aortic corner then pass through the gap between leaflet's earing and hinge recess and exit the ventricle corner. The platelets moving through these streamlines will travel the longest distance and thus experience a longer exposure time under the elevated shear stress (in the hinge recess). The platelet activation on the plane of 300 μm above the flat is also shown in Fig. 6 for the Soares model. The activation in this plane mainly happens due to the jet from the b-datum gap. The maximum velocity and shear of 2.8 m/s and 1200 dyne/cm^2 can be seen on this plane (Figs. 2c and 4a).

The total activation depends on both the shear stress and the number of platelets exposed to shear stress, i.e., flow rate during diastole. In the diastole, during the rapid closure of the leaflets ($t = 430$ ms), there is a sharp increase in the total platelet activation because of the high flow rate of the leakage flow (Fig. 5). After the valves close, the flow rate through the hinge and b-datum gap is almost constant (see the flow curve in Fig. 5). Consequently, the rate of activation in this phase is not changing much and the total activation is almost linear in this phase.

Based on the above discussion, even though the platelets in hinge region are exposed to much higher shear stress levels (compare Figs. 4 and 7) and locally show higher levels of activation (compare Figs. 6 and 8), the total amount of activation generated by hinge domain is less than 20% of the bulk domain mainly because of the low flow rate through the hinge domain compared to the bulk flow (Fig. 5). In fact, the mean flow rate of the leakage flow after the valve closure through the hinge region and b-datum gap is only about 2% of the forward flow rate through the valve in the bulk flow (Fig. 5). Therefore, a considerably smaller number of platelets will be exposed to high shear during diastole compared to the bulk flow, which is the main reason for the lower total amount of activation generated in the hinge region (Fig. 5).

4. Conclusion

In this study, we developed a numerical framework which enables us to answer the open question about the role of systole phase (bulk flow) versus diastole phase (hinge/gap flow) in the poor thrombogenic performance of BMHVs in terms of shear induced platelet activation. The results show that while the hinge area has a higher shear stress and maximum local activation compared to the bulk flow, the total activation due to the bulk flow, contrary to the common belief (Simon et al., 2010b; Ellis et al., 1996; Jun et al., 2014a), is several times higher than that of hinge/leakage flow using both activation models. This is mainly because of the higher flow rate during systole exposes more platelets to elevated shear in the bulk flow, whereas the low leakage flow rate during diastole (~2% of bulk flow at peak systole) exposes lower number of platelets to much higher shear stress. The relative importance of the amount of platelets exposed (flow rate) vs. the elevated shear and exposure time was ignored in the previous studies.

Comparing the results of one-way and two-way interpolation with the experiments (Simon et al., 2004; Jun et al., 2014a), shows that, although most of the previous numerical simulation (Simon et al., 2010a,b; Yun et al., 2012) has used one-way interpolation due to computational simplicity, the results using this method will overestimates the velocities, shear stress, and the platelet activation during the diastole phase in the hinge region. In addition, our results show that the hinge gap size can significantly affect the washout potential of BMHVs while the maximum shear stress and total activation do not change remarkably (less than 10%) for different hinge gap sizes. The larger gap size shows a better washout performance near the hinge region by having a higher maximum instantaneous velocity through the hinge (2.8 m/s) in comparison to the smaller one (2.4 m/s).

5. Limitations

The limitation of our study is that the simulations were performed for only one cardiac cycle and no region with activation higher than Hellums criterion (35 dyne s/cm^2) or $\Delta PAS = 1$ was identified during one time passage. Nevertheless, such levels of activation can be reached after multiple passages through the valves. The implicit assumption of our comparison of total platelet activation in hinge vs. bulk flow, therefore, is that every passage generates similar activation in each region. This is a reasonable assumption as the cycle-to-cycle variations of the flow in mechanical valves are small (Dasi et al., 2007), i.e., similar flow field in each cycle, which creates similar shear exposure to platelets in consecutive cycles. In addition, due to the complexity of platelet activation phenomenon, any mathematical model for predicting activation is limited to its range of verified validity and its assumptions (from simplifying assumptions in the experiments to neglecting chemical factors in platelet activation).

Conflict of interest

The authors declare that there is no conflict of interest regarding the publication of this article.

Acknowledgments

This work was supported by American Heart Association grant 13SDG17220022 and the Center of Computational Research (CCR) of University at Buffalo.

Appendix A. Supplementary material

Supplementary data associated with this article can be found, in the online version, at https://doi.org/10.1016/j.jbiomech.2018.12.003.

References

Alemu, Y., Bluestein, D., 2007. Flow-induced platelet activation and damage accumulation in a mechanical heart valve: numerical studies. Artif. Organs 31 (9), 677–688.
Alemu, Y., Girdhar, G., Xenos, M., Sheriff, J., Jesty, J., Einav, S., Bluestein, D., 2010. Design optimization of a mechanical heart valve for reducing valve thrombogenicity–a case study with ATS valve. ASAIO J. 56 (5), 389–396.
Asgharzadeh, H., Borazjani, I., 2017. A Newton–Krylov method with an approximate analytical jacobian for implicit solution of Navier–Stokes equations on staggered overset-curvilinear grids with immersed boundaries. J. Comput. Phys. 331, 227–256.
Bluestein, D., Niu, L., Schoephoerster, R.T., Dewanjee, M.K., 1997. Fluid mechanics of arterial stenosis: relationship to the development of mural thrombus. Ann. Biomed. Eng. 25 (2), 344–356.
Bluestein, D., Yin, W., Affeld, K., Jesty, J., 2004. Flow-induced platelet activation in a mechanical heart valve. J. Heart Valve Dis. 13 (3), 501–508.
Borazjani, I., 2013. Fluid–structure interaction, immersed boundary-finite element method simulations of bio-prosthetic heart valves. Comput. Methods Appl. Mech. Eng. 257, 103–116.
Borazjani, I., Ge, L., Le, T., Sotiropoulos, F., 2013. A parallel overset-curvilinear-immersed boundary framework for simulating complex 3d incompressible flows. Comput. Fluids 77, 76–96.
Borazjani, I., Ge, L., Sotiropoulos, F., 2008. Curvilinear immersed boundary method for simulating fluid structure interaction with complex 3d rigid bodies. J. Comput. Phys. 227 (16), 7587–7620.
Clark, M.A., Duhay, F.G., Thompson, A.K., Keyes, M.J., Svensson, L.G., Bonow, R.O., Stockwell, B.T., Cohen, D.J., 2012. Clinical and economic outcomes after surgical aortic valve replacement in medicare patients. Risk Manage. Healthcare Policy 5, 117.
Dasi, L., Ge, L., Simon, H., Sotiropoulos, F., Yoganathan, A., 2007. Vorticity dynamics of a bileaflet mechanical heart valve in an axisymmetric aorta. Phys. Fluids 19 (6), 067105.
Dumont, K., Vierendeels, J., Kaminsky, R., Van Nooten, G., Verdonck, P., Bluestein, D., 2007. Comparison of the hemodynamic and thrombogenic performance of two bileaflet mechanical heart valves using a CFD/FSI model. J. Biomech. Eng. 129 (4), 558–565.
Ellis, J., Healy, T., Fontaine, A., Saxena, R., Yoganathan, A., 1996. Velocity measurements and flow patterns within the hinge region of a medtronic parallel bileaflet mechanical valve with clear housing. J. Heart Valve Disease 5 (6), 591–599.
Ellis, J.T., Travis, B.R., Yoganathan, A.P., 2000. An in vitro study of the hinge and near-field forward flow dynamics of the st. jude medical® regent bileaflet mechanical heart valve. Ann. Biomed. Eng. 28 (5), 524–532.
Fallon, A.M., Shah, N., Marzec, U.M., Warnock, J.N., Yoganathan, A.P., Hanson, S.R., 2006. Flow and thrombosis at orifices simulating mechanical heart valve leakage regions. J. Biomech. Eng. 128 (1), 30–39.
Ge, L., Sotiropoulos, F., 2007. A numerical method for solving the 3d unsteady incompressible Navier–Stokes equations in curvilinear domains with complex immersed boundaries. J. Comput. Phys. 225 (2), 1782–1809.
Gilmanov, A., Sotiropoulos, F., 2005. A hybrid cartesian/immersed boundary method for simulating flows with 3d, geometrically complex, moving bodies. J. Comput. Phys. 207 (2), 457–492.
Grigioni, M., Daniele, C., Morbiducci, U., DAvenio, G., Di Benedetto, G., Barbaro, V., 2004. The power-law mathematical model for blood damage prediction: analytical developments and physical inconsistencies. Artif. Organs 28 (5), 467–475.
Hanafizadeh, P., Mirkhani, N., Davoudi, M.R., Masouminia, M., Sadeghy, K., 2016. Non-newtonian blood flow simulation of diastolic phase in bileaflet mechanical heart valve implanted in a realistic aortic root containing coronary arteries. Artif. Organs 40 (10).
Hedayat, M., Asgharzadeh, H., Borazjani, I., 2017. Platelet activation of mechanical versus bioprosthetic heart valves during systole. J. Biomech. 56, 111–116.
Hosseinzadegan, H., Tafti, D.K., 2017. Modeling thrombus formation and growth. Biotechnol. Bioeng.
Iung, B., Vahanian, A., 2011. Epidemiology of valvular heart disease in the adult. Nat. Rev. Cardiol. 8 (3), 162–172.
Jesty, J., Bluestein, D., 1999. Acetylated prothrombin as a substrate in the measurement of the procoagulant activity of platelets: elimination of the feedback activation of platelets by thrombin. Anal. Biochem. 272 (1), 64–70.
Jun, B.H., Saikrishnan, N., Arjunon, S., Yun, B.M., Yoganathan, A.P., 2014a. Effect of hinge gap width of a st. jude medical bileaflet mechanical heart valve on blood damage potential–an in vitro micro particle image velocimetry study. J. Biomech. Eng. 136 (9), 091008.
Jun, B.H., Saikrishnan, N., Yoganathan, A.P., 2014b. Micro particle image velocimetry measurements of steady diastolic leakage flow in the hinge of a st. jude medical® regent mechanical heart valve. Ann. Biomed. Eng. 42 (3), 526–540.

Klusak, E., Bellofiore, A., Loughnane, S., Quinlan, N.J., 2015. High-resolution measurements of velocity and shear stress in leakage jets from bileaflet mechanical heart valve hinge models. J. Biomech. Eng. 137 (11), 111008.

Kuan, Y.H., Kabinejadian, F., Nguyen, V.-T., Su, B., Yoganathan, A.P., Leo, H.L., 2015. Comparison of hinge microflow fields of bileaflet mechanical heart valves implanted in different sinus shape and downstream geometry. Comput. Methods Biomech. Biomed. Eng. 18 (16), 1785–1796.

Lamson, T.C., Rosenberg, G., Geselowitz, D.B., Deutsch, S., Stinebring, D.R., Frangos, J. A., Tarbell, J.M., 1993. Relative blood damage in the three phases of a prosthetic heart valve flow cycle. Asaio J. 39 (3), M626–M633.

Leo, H., Simon, H.A., Dasi, L.P., Yoganathan, A.P., 2006. Effect of hinge gap width on the microflow structures in 27-mm bileaflet mechanical heart valves. J. Heart Valve Dis. 15 (6), 800.

Leo, H.-L., He, Z., Ellis, J.T., Yoganathan, A.P., 2002. Microflow fields in the hinge region of the carbomedics bileaflet mechanical heart valve design. J. Thorac. Cardiovasc. Surg. 124 (3), 561–574.

Manning, K.B., Kini, V., Fontaine, A.A., Deutsch, S., Tarbell, J.M., 2003. Regurgitant flow field characteristics of the st. jude bileaflet mechanical heart valve under physiologic pulsatile flow using particle image velocimetry. Artif. Organs 27 (9), 840–846.

Morbiducci, U., Ponzini, R., Nobili, M., Massai, D., Montevecchi, F.M., Bluestein, D., Redaelli, A., 2009. Blood damage safety of prosthetic heart valves. Shear-induced platelet activation and local flow dynamics: a fluid–structure interaction approach. J. Biomech. 42 (12), 1952–1960.

Nobili, M., Sheriff, J., Morbiducci, U., Redaelli, A., Bluestein, D., 2008. Platelet activation due to hemodynamic shear stresses: damage accumulation model and comparison to in vitro measurements. ASAIO J. (Am. Soc. Artif. Internal Organs: 1992) 54 (1), 64.

Ross, D.W., Ayscue, L.H., Watson, J., Bentley, S.A., 1988. Stability of hematologic parameters in healthy subjects: intraindividual versus interindividual variation. Am. J. Clin. Pathol. 90 (3), 262–267.

Sheriff, J., Soares, J.S., Xenos, M., Jesty, J., Bluestein, D., 2013. Evaluation of shear-induced platelet activation models under constant and dynamic shear stress loading conditions relevant to devices. Ann. Biomed. Eng. 41 (6), 1279–1296.

Simon, H.A., Ge, L., Borazjani, I., Sotiropoulos, F., Yoganathan, A.P., 2010a. Simulation of the three-dimensional hinge flow fields of a bileaflet mechanical heart valves under physiologic conditions. Ann. Biomed. Eng. 38 (3), 1257.

Simon, H.A., Ge, L., Sotiropoulos, F., Yoganathan, A.P., 2010b. Numerical investigation of the performance of three hinge designs of bileaflet mechanical heart valves. Ann. Biomed. Eng. 38 (11), 3295–3310.

Simon, H.A., Leo, H.-L., Carberry, J., Yoganathan, A.P., 2004. Comparison of the hinge flow fields of two bileaflet mechanical heart valves under aortic and mitral conditions. Ann. Biomed. Eng. 32 (12), 1607–1617.

Soares, J.S., Sheriff, J., Bluestein, D., 2013. A novel mathematical model of activation and sensitization of platelets subjected to dynamic stress histories. Biomech. Model. Mechanobiol. 12 (6), 1127–1141.

Suri, R.M., Schaff, H.V., 2013. Is tissue valve the preferred option for patients aged 60 years and older? Selection of aortic valve prostheses: contemporary reappraisal of mechanical versus biologic valve substitutes. Circulation 128 (12), 1372–1380.

Tang, G.H., Rao, V., Siu, S., Butany, J., 2005. Thrombosis of mechanical mitral valve prosthesis. J. Cardiac Surg. 20 (5), 481–486.

Travis, B.R., Marzec, U.M., Leo, H.L., Momin, T., Sanders, C., Hanson, S.R., Yoganathan, A.P., 2001. Bileaflet aortic valve prosthesis pivot geometry influences platelet secretion and anionic phospholipid exposure. Ann. Biomed. Eng. 29 (8), 657–664.

Xenos, M., Girdhar, G., Alemu, Y., Jesty, J., Slepian, M., Einav, S., Bluestein, D., 2010. Device thrombogenicity emulator (DTE)- design optimization methodology for cardiovascular devices: a study in two bileaflet MHV designs. J. Biomech. 43 (12), 2400–2409.

Yin, W., Alemu, Y., Affeld, K., Jesty, J., Bluestein, D., 2004. Flow-induced platelet activation in bileaflet and monoleaflet mechanical heart valves. Ann. Biomed. Eng. 32 (8), 1058–1066.

Yun, B.M., Aidun, C.K., Yoganathan, A.P., 2014a. Blood damage through a bileaflet mechanical heart valve: a quantitative computational study using a multiscale suspension flow solver. J. Biomech. Eng. 136 (10), 101009.

Yun, B.M., McElhinney, D.B., Arjunon, S., Mirabella, L., Aidun, C.K., Yoganathan, A.P., 2014b. Computational simulations of flow dynamics and blood damage through a bileaflet mechanical heart valve scaled to pediatric size and flow. J. Biomech. 47 (12), 3169–3177.

Yun, B.M., Wu, J., Simon, H.A., Arjunon, S., Sotiropoulos, F., Aidun, C.K., Yoganathan, A.P., 2012. A numerical investigation of blood damage in the hinge area of aortic bileaflet mechanical heart valves during the leakage phase. Ann. Biomed. Eng. 40 (7), 1468–1485.

Zhang, P.S. H., Dalal, A.R., Kresh, J.Y., Laub, G.W., 2016. A novel technique for experimental flow visualization of mechanical valves. ASAIO J. 62 (2), 133–138.